Kinetics of joint ordering and decomposition in binary alloys

V. I. Gorentsveig
Departments of Physics and Mathematics, Rutgers University, New Brunswick, New Jersey 08903

P. Fratzl
Institut für Materialphysik, Universität Wien, Boltzmanngasse 5, A-1090 Wien, Austria

J. L. Lebowitz
Departments of Physics and Mathematics, Rutgers University, New Brunswick, New Jersey 08903
(Received 2 August 1996)

We study phase segregation in a model alloy undergoing both ordering and decomposition, using computer simulations of Kawasaki exchange dynamics on a square lattice. Following a quench into the miscibility gap we observe an early stage in which ordering develops while the composition remains almost uniform. Then decomposition starts with segregation into ordered and disordered phases. The two spherically averaged structure functions, related to decomposition and to ordering, were both observed to obey scaling rules in the late coarsening stage where the time increase of the characteristic lengths was consistent with $a(t^{1/3}+b)$. While a was similar for ordering and decomposition at low concentration of the minority component, it showed an increase (decrease) with concentration for ordering (decomposition). The domain morphology was found to depend on the concentration of the minority component, in a way that suggests a wetting of antiphase boundaries in the ordered domains by the disordered phase. [S0163-1829(97)03005-1]

I. INTRODUCTION

The kinetics of alloy decomposition is a theoretically challenging and technologically important problem that has attracted much attention over many years.[1–6] For alloy systems where the lattice spacings in matrix and precipitate are the same, and the two-phase structure coarsens with time to reduce its interfacial energy, both the morphology and the growth rate of the domains seem to have a universal behavior.[7] In such systems, the typical domain size grows asymptotically with time t like a power t^{α}, $\alpha=1/3$,[8,9] and the essential features of the morphology depend only on the volume fraction f of precipitates.[9,10]

This ''universal'' morphology is known to break down in cases where the lattice spacings are different in matrix and precipitates. The so-induced elastic misfit interactions may change the morphology as well as the kinetics of the decomposition. Such systems have been the subject of numerous experimental[11–16] and theoretical[17–26] studies in recent years. It has been found that anisotropic elastic constants lead to the formation of very anisotropic, mostly platelike precipitates. Nevertheless, their typical size still grows in many cases like $t^{1/3}$,[24,15] remaining so even under externally applied stresses.[25]

An interesting situation occurs in cases where the precipitates are ordered intermetallic alloys, such as in Al-Li or in nickel-based superalloys. Here the decomposition (described by the conserved order parameter c, that is the local concentration of A atoms in the A-B alloy) couples to an ordering transition (described by a nonconserved order parameter). In Ni-based superalloys both the ordering of the precipitates and the elastic misfit interactions will be present.[11–15] Recent computer work[19,20,26,27] is devoted to the study of models that include both effects. While some features of the morphology, like the cuboidal shape of the precipitates and their predominant alignment along certain crystallographic directions, are clearly due to the elastic misfit interactions, some other features are probably due to the ordering of the precipitates. Indeed, it is usually found in these alloys that close neighboring precipitates do not merge even though this would reduce the total surface energy.[11–15] A possible explanation, proposed in Ref. 20, is that these precipitates belong to different variants of the same ordered structure so that their merging would lead initially to an antiphase boundary (APB), whose energy is higher than that of the interfaces between the ordered precipitates and the disordered matrix.

In order to address this issue and to gain a better understanding of the influence of atomic ordering on the coarsening kinetics and morphology, we have carried out computer simulations of an Ising model on a square lattice with nearest- and next-nearest-neighbor interactions, which does not include elastic misfit interactions. There will now be two variants of the ordered phase depending on which sublattice is occupied by which type of atoms and if a wetting of APB's by the disordered phase reduces the total energy, then the domain morphology will be very different from the case where none of the phases (minority or majority) is ordered. In particular, at larger volume fractions f of the ordered phase, e.g., when $f>0.5$, APB's are to be expected between the differently ordered domains. It is unclear whether the length scale of precipitates in such a system will still grow like $t^{1/3}$ or will behave like $t^{1/2}$, the typical growth law for nonconserved quantities.

The model we investigate was studied previously by Sahni *et al.*[28] Their conclusions were mainly qualitative. In the present work we extend their simulations and obtain more quantitative information about the joint kinetics of ordering and segregation. We concentrate on comparing the

growth kinetics and morphology at $f<0.5$, $f=0.5$ and $f>0.5$ with those obtained for an alloy where none of the phases has an ordered intermetallic structure. While the $t^{1/3}$ law appears to hold in all cases, the coefficient a has very different dependence on concentration for the ordering and segregation, the former growing much faster for higher concentrations. We also find, in the case of high volume fraction of ordered precipitates, clear evidence of the wetting of APB's. This may explain some of the results in Al-Li systems[29,30] where ordered domains with little lattice mismatch are formed and supports the interpretation of nonmerging precipitates given in Refs. 29 and 30. We plan to extend our work to include elastic interactions, present in Ni-based alloys,[11–15] mentioned earlier.

II. THE MODEL

We consider an Ising model on a two-dimensional (2D) square lattice with nearest-neighbor interactions J of the antiferromagnetic type and next-nearest-neighbor interactions of the ferromagnetic type, which in our simulations we took to be $-J/2$. The total energy U of this system, wrapped on a torus containing $N=L^2$ sites, is

$$U=J\sum_{\langle \mathbf{l},\mathbf{l}'\rangle_+}\sigma_{\mathbf{l}}\sigma_{\mathbf{l}'}-\frac{1}{2}J\sum_{\langle \mathbf{l},\mathbf{l}'\rangle_\times}\sigma_{\mathbf{l}}\sigma_{\mathbf{l}'},\quad J>0, \tag{1}$$

where $\sigma_{\mathbf{l}}=1$ if there is an A atom and $\sigma_{\mathbf{l}}=-1$ if there is a B atom, on the lattice site $\mathbf{l}=(\mathbf{l_1},\mathbf{l_2})$ and the first and the second sums are over all nearest- and next-nearest-neighbor pairs, respectively. The average concentration c of minority B atoms is

$$c=(1-\overline{\sigma})/2,$$

where

$$\overline{\sigma}=\frac{1}{N}\sum_{\mathbf{l}}\sigma_{\mathbf{l}}.$$

The phase diagram of this system obtained from Monte Carlo simulation[31,32] is shown schematically in Fig. 1. The critical point for the ordering transition is at $c_c=0.5$ and $T_c\simeq 3.8J/k$ and there is a tricritical point at $c_i\simeq 0.27$ and $T_t\simeq 1.3J/k$. Above T_t the transition between the disordered A-rich phase and the ordered phase is of second order, while below T_t the transition is of first order. Figure 1 shows the miscibility gap between the ordered phase (with practically stoichiometric A-B composition) and the disordered phase.

Our simulations were performed on a square lattice, 128×128, with periodic boundary conditions, at $T=0.9J/k$ at three values for the composition, $c=0.15$, 0.25, and 0.35. These are all well within the two-phase region of Fig. 1 between the ordered intermetallic alloy with stoichiometric composition AB and the disordered A-rich phase; corresponding approximately to volume fractions of ordered phase of about $f=0.3$, 0.5, and 0.7, respectively. The dynamics of the ordering/decomposition process, which are our main concern, were followed using Kawasaki dynamics with the Metropolis rule, that is by choosing a nearest-neighbor pair at random and then exchanging the atoms with probability

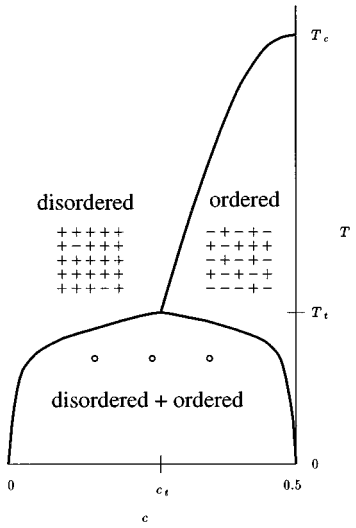

FIG. 1. Schematic equilibrium phase diagram (concentration of B atoms c vs temperature T) for the model A-B alloy. The circles show the conditions at which our computer experiments were performed.

$$\omega=\min[1,\exp(-\Delta U/kT)],$$

where ΔU is the change in the total energy U given by Eq. (1).

In our simulations we start the realizations (computer runs) from randomly generated ''infinite'' temperature configurations. Time is then measured in Monte Carlo Steps (MCS), that is the number of attempted nearest-neighbor exchanges per lattice site.

III. CHARACTERIZATION OF CONFIGURATIONS

Since there are two sublattices within the ordered ''antiferromagnetic'' structure on the square lattice, there will also be two possible variants for the ordered phase, one where the A atoms are on the even sublattice (which we call for short the even variant) and one where the A atoms are on the odd sublattice (odd variant). To represent ''snapshot'' pictures of the configurations in a way that clearly differentiates between the two variant ordered phases as well as the disordered phase, we use the following variable:

$$\eta_{\mathbf{l}}=\frac{1}{2}\left(\sigma^s_{\mathbf{l}}+\frac{1}{4}\sum_{\langle \mathbf{l}'\rangle^+_{\mathbf{l}}}\sigma^s_{\mathbf{l}'}\right), \tag{2}$$

where the sum is over nearest-neighboring sites, and

$$\sigma^s_{\mathbf{l}}=(-1)^{l_1+l_2}\sigma_{\mathbf{l}}$$

is the staggered spin. The variable $\eta_{\mathbf{l}}$ takes the value -1 at sites within ordered domains of the odd variant and $+1$ on sites within ordered domains of the even variant. In the disordered phase, where almost all atoms are of the same kind, $\eta_{\mathbf{l}}=0$. Intermediate values $\eta_{\mathbf{l}}=\pm 1/4,\ \pm 1/2,\ \pm 3/4$ appear on the interfaces between ordered and disordered domains and at isolated B atoms dissolved in the A-rich (disordered) phase. Translating this into a gray scale, the two variants of

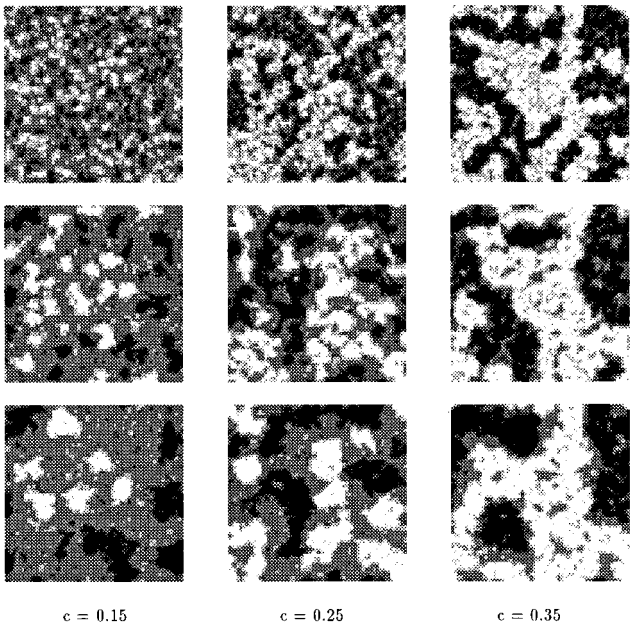

FIG. 2. Plots of configurations of the local order parameter $\eta_{\mathbf{l}}$ (by means of brightness $\eta_{\mathbf{l}}=-1$ being white ane $\eta_{\mathbf{l}}=+1$ being black), at three time points, $t^{1/3}=5$, 20, 40 (time, t in units of MCS, from top to bottom) for each of three concentrations, $c=0.15$, 0.25, and 0.35. The disordered phase has $\eta_{\mathbf{l}}\approx 0$ and appears gray. The lattice size is 128×128.

the ordered phases appear black and white, respectively, while the disordered phase appears in gray, see Fig. 2.

The staggered spin-local average $\eta_{\mathbf{l}}$ can be interpreted as local order parameter for ordering and its absolute value averaged over the lattice,

$$\eta_{\rm sr}\equiv|\overline{\eta}|=\frac{1}{N}\sum_{\mathbf{l}}\ |\eta_{\mathbf{l}}| \tag{3}$$

can be considered as a short-range order parameter (for the atomic ordering, as opposed to decomposition). It represents the relative amount of ordered phase, irrespective of whether the order corresponds to the odd or the even variant.

The average over the entire lattice of the staggered spin local average,

$$\eta_{lr}\equiv\overline{\eta}=\frac{1}{N}\sum_{\mathbf{l}}\ \eta_{\mathbf{l}}=\frac{1}{N}\sum_{\mathbf{l}}\ \sigma_{\mathbf{l}}^{s}, \tag{4}$$

is equal to the global average of the staggered spin variable and can be considered as a long-range order parameter. It corresponds to twice the difference in the concentration of A atoms between the odd and the even sublattice. Similar order parameters may also be defined for decomposition, although their interpretation is more ambiguous now,

$$\rho_{\rm sr}\equiv\frac{1}{N}\sum_{\mathbf{l}}\ |\rho_{\mathbf{l}}|,\quad \rho_{\rm lr}\equiv\frac{1}{N}\sum_{\mathbf{l}}\ \rho_{\mathbf{l}}=1-2c, \tag{5}$$

where

$$\rho_{\mathbf{l}}=\frac{1}{2}\left(\sigma_{\mathbf{l}}+\frac{1}{4}\sum_{\langle\mathbf{l}'\rangle_{\mathbf{l}}^{+}}\ \sigma_{\mathbf{l}'}\right).$$

From these definitions it is apparent that the long-range order parameter $\rho_{\rm lr}$ for decomposition is conserved (since c is fixed) while $\eta_{\rm lr}$ is nonconserved. One may further notice that an alternative way to write $\eta_{\rm sr}$ is

$$\eta_{\rm sr}=1-\rho_{\rm sr}=\frac{1}{2}-\frac{1}{4N}\sum_{\langle\mathbf{l},\mathbf{l}'\rangle_{+}}\ \sigma_{\mathbf{l}}\sigma_{\mathbf{l}'}=2c(1-c)(1-\alpha_1). \tag{6}$$

This expression shows that $\eta_{\rm sr}$ is related linearly to the first Warren-Cowley short-range order parameter α_1 generally used in crystallography,[33]

$$\alpha_1=1-p^{AB}/c,$$

where p^{AB} is the density of B atoms at nearest-neighbor sites of an A atom. To characterize the decomposition kinetics, we use the structure function

$$S_{\mathbf{k}}=\frac{1}{N}\left|\sum_{\mathbf{l}}\ \exp(i\mathbf{k}\cdot\mathbf{l})\sigma_{\mathbf{l}}\right|^2, \tag{7}$$

where $\mathbf{k}=(k_1,k_2)$ is a reciprocal-lattice vector, with $k_j=2\pi K_j/L$ and $K_j=1,2,\ldots,L$ for $j=1,2$. For the system undergoing both ordering and decomposition, the structure function (shown in Fig. 3 by means of brightness) is localizing in two areas, around the point (π,π) (related to ordering) and around the point (0,0) (related to decomposition) of reciprocal space. Note, that $S_{(0,0)}=N\rho_{\rm lr}^2$ and that $S_{(\pi,\pi)}=N\eta_{\rm lr}^2$.

To study kinetics and scaling properties of the two processes we divide the (square-shaped) Brillouin zone in reciprocal space in two equal areas (bold lines in Fig. 3): the square for ordering,

$$\Omega_{\pi}=\{\mathbf{k}:|k_1-\pi|+|k_2+\pi|\leqslant\pi\} \tag{8}$$

(that is inside that boundary in Fig. 3) and the remaining four quarters of the square for decomposition. Using the periodicity of the reciprocal lattice, the latter can be put together as a square,

$$\Omega_0=\{\mathbf{k}:|k_1|+|k_2|\leqslant\pi\} \tag{9}$$

shown separately in Fig. 3 with higher resolution for values of the structure function. To test scaling behavior of the structure function, we sphericalize it within the two squares Ω_ν related to ordering $(\nu=\pi)$ and to decomposition $(\nu=0)$, separately. We define

$$S_\nu(k)=\sum_{\Delta_\nu(k)}\ S_{\mathbf{k}'}\Big/\sum_{\Delta_\nu(k)}\ 1, \tag{10}$$

where

$$\Delta_\nu(k)=\{\mathbf{k}':k-\delta k<|\mathbf{k}'-(\nu,\nu)|\leqslant k+\delta k\}$$

is a ring of width $2\delta k$ and median radius $k=|\mathbf{k}|=(k_1^2+k_2^2)^{1/2}$, centered at (ν,ν). The sphericalized structure function was actually computed for the values $k=2\pi K/L$, K being an integer: $K=1,2,\ldots,[L/2\sqrt{2}]$, and choosing $\delta k=\pi/L$. Since the configurations on the lattice are evolving with time, we are also using the notation $S_\nu(k,t)$ for the sphericalized structure function computed for the configuration at time t.

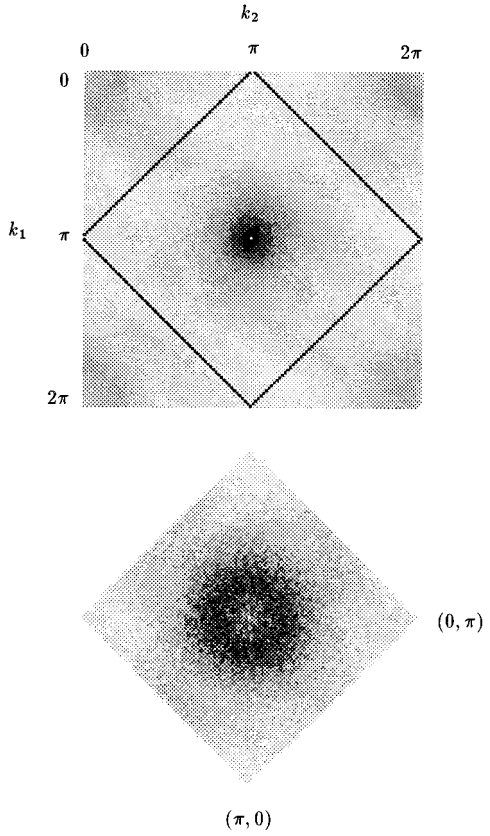

FIG. 3. Plot (by means of brightness, black meaning high values) of the structure function, $S_{\mathbf{k}}$, in the entire Brillouin zone (top) and in its parts related to decomposition (bottom, with higher contrast) at $t^{1/3}=5$ (time, t is given in units of MCS), for the concentration $c=0.25$.

The scaling hypothesis for the late stages of coarsening, in systems undergoing either phase segregation or ordering, is that the system is characterized by a single scale $\lambda(t)$. This means in particular that for values of k^{-1} which are large compared to the lattice spacing and small compared to the size of the system $S(k,t)$ should (up to a time-dependent factor) be a function of only one variable, $\lambda(t)k$. In our case we need *a priori* two characteristic lengths, $\lambda_\nu(t)$, $\nu=0,\pi$. We therefore hypothesize that for the system under consideration

$$\widetilde{S}_\nu(k,t)\approx A_\nu(t)F_\nu(k\lambda_\nu(t)) \quad \text{as} \quad t\to\infty, \tag{11}$$

where $\widetilde{S}_\nu(k,t)$ is the macroscopic, formally the infinite volume limit, for fixed $k\neq 0$, of the corresponding sphericalized structure function at time t:[9]

$$S_\nu(k,t)\to\widetilde{S}_\nu(k,t) \quad \text{as} \quad L\to\infty.$$

We shall show, in Sec. IV, that this generalized scaling hypothesis is indeed consistent with our simulation data.

One of the common ways of defining a characteristic length is to use inverse moments of the structure function. Since we are restricted in simulations to systems which are very small on the macroscopic scale, great care has to be taken in computing from the available data quantities relevant for macroscopic systems. This is doubly so for our system where we have both ordering and segregation. We therefore had to find a way which minimizes distortions of the time dependence of the λ_ν due to the finite size of the system. To achieve this we defined the moments

$$k_\nu(t)=\sum_{k_a}^{k_b} k^{1+r_\nu}S_\nu(k,t) \Big/ \sum_{k_a}^{k_b} k^{r_\nu}S_\nu(k,t) \tag{12}$$

with $r_0=1$ and $r_\pi=2$, where the limits of summation, k_a and k_b, were themselves scaled in accordance with $k_\nu(t)$, by setting $k_{a,b}(t)=(1\pm h)k_\nu(t)$; so at different times the moments are calculated from similar intervals. Taking $h=0.7$, the interval around k_ν was large enough to give sufficient statistics for the summation, but still small enough to avoid any contribution from the structure function at very small or very large k, which might be affected by finite-size effects. The $k_\nu(t)$ so obtained appeared to follow the position of the maximum of $k^{r_\nu}S_\nu(k,t)$ in Eq. (12).

With the procedure described above, finite-size effects on $k_\nu(t)$ could be minimized. Indeed, additional runs performed on a smaller lattice (64×64) gave consistent results for the time evolution of $k_\nu(t)$. Of course this still leaves considerable uncertainties in determining $k_\nu(t)$. For the size of system we are dealing with, the gaps in the k's, which are equal to $2\pi/L$, limit any finer resolution independent of the number or duration of the runs.

IV. RESULTS

Snapshot pictures of typical configurations obtained at $T=0.9J/k$ for alloy compositions $c=0.15$, 0.25, and 0.35 with lattice size $L=128$ are shown in Fig. 2. The value for the locally averaged spin $\eta_{\mathbf{l}}$, defined in Eq. (2) is shown at 125, 8000, and 64 000 MCS. Three different types of domains appear in these pictures in white, black, and gray corresponding to ordered phases on the even and the odd sublattice and the disordered A-rich phase, respectively. In the case $c=2.5$, the gray phase covers about half of the specimen volume, while at $c=0.35$ it covers less and at $c=0.15$ more. This is, as already mentioned, in qualitative agreement with the equilibrium phase diagram,[28,31,32] where the predicted volume fractions of black or white (that is ordered) phase are $f=0.3$, 0.5, and 0.7 for $c=0.15$, 0.25, and 0.35, respectively, see Fig. 1. In the case of decomposition without ordering, when the miscibility gap is symmetric around the critical composition, the behavior of an alloy with $f=0.3$ would be identical to the one at $f=0.7$, with the two phases exchanged in their respective role. In the present case, however, it becomes clear from looking at Fig. 2 that there is a completely different behavior on different sides of the tricritical composition. At $c=0.15$ the pictures show isolated ordered droplets within a disordered matrix, while for $c=0.35$ they show the disordered phase surrounding the ordered domains, i.e., we see an ordered alloy with the antiphase boundaries between the two ordered variants wetted by the disordered phase.

A. Early stage behavior

We observe that the short-range order parameter η_{sr} comes rapidly to the steady value $2c$, corresponding to complete ordering. We find that the relative deviation becomes

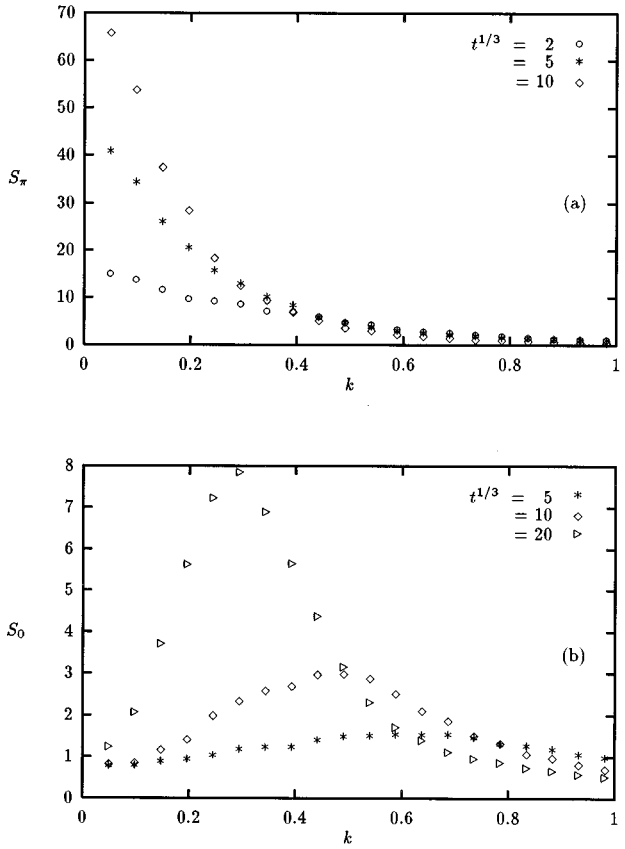

FIG. 4. (a) Plots of the spherically averaged structure function for ordering, $S_\pi(k)$, at $t^{1/3}=2$, 5, 10 (time, t is given in units of MCS) for concentration $c=0.25$. (b) $S_0(k)$ at times $t^{1/3}=5$, 10, 20.

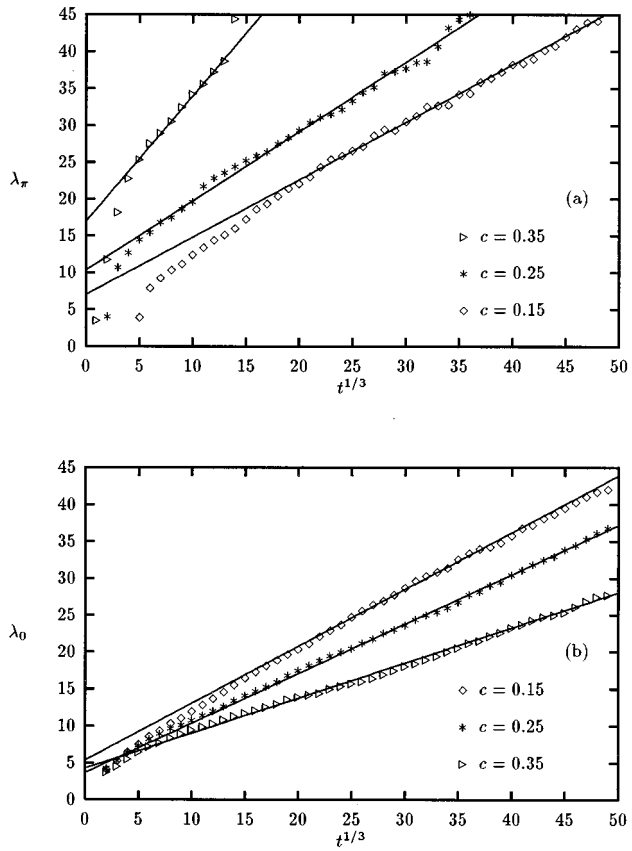

FIG. 5. Dependence of the characteristic wave length for (a) ordering, λ_π, and (b) decomposition, λ_0, on time, t (in units of MCS) at three concentrations: $c=0.15$ (diamonds), 0.25 (stars), and 0.35 (triangles).

small, $|\eta_{\rm sr}/2c-1|\leqslant 10^{-2}$, by the time $t\approx 10^2$, indicating that local ordering is well developed by that time. At the same time a domain structure starts to be visible (see Fig. 2). Ordered domains of both kinds (even and odd variant) occur in about equal fractions. Domains of pure minority component are practically not observed (in the original spin configuration) after time $t\sim 10^2$. Then segregation of ordered and majority phases develops.

We further observe that the sphericalized structure function for ordering, $S_\pi(k)$, develops a maximum localized at $k\sim 0$ by the time $t\sim 10$ (starting from times $t\sim 1$) which grows sharper as t increases [Fig. 4(a)], while the sphericalized structure function for decomposition, $S_0(k)$, develops a maximum at $k\sim k_0$ later, starting at $t\sim 10^2$ [Fig. 4(b)]. This shows, in agreement with what was found in Refs. 29, 30, and 34, that, initially, ordering is much faster than decomposition.

Moreover, the sum of the structure function components related to ordering

$$Ns_\pi=\sum_{\Omega_\pi} S_{\mathbf{k}} \tag{13}$$

approaches the constant value $2Nc$, which corresponds to the area of ordered phase at complete phase separation. Similarly, the sum of the structure function components related to decomposition (that is, within the square Ω_0 with exclusion of the origin),

$$Ns_0=\sum_{\Omega_0'} S_{\mathbf{k}} \tag{14}$$

also reaches a steady value Ns_0^c, with $s_0^c\simeq(1-2c)2c$, which was to be expected, since there is a general relation between s_0 and s_π:

$$s_\pi+s_0=1-S_{(0,0)}/N=4c(1-c). \tag{15}$$

The relative deviation of s_0 from its equilibrium value, $|s_0/s_0^c-1|$, becomes smaller than 10^{-2}, for times $t>10^2$.

B. Scaling analysis

As already mentioned, both spherical averages of the structure functions, $S_\pi(k)$, and $S_0(k)$ defined in Eq. (10),

TABLE I. Parameters a_ν and b_ν characterizing the growth Eq. (16) of the characteristic lengths defined in Eq. (12), at different concentrations c of minority component.

c	a_π	b_π	a_0	b_0
0.15	0.78	9.0	0.77	7.0
0.25	0.94	11.0	0.67	5.5
0.35	1.7	10.0	0.475	9.0

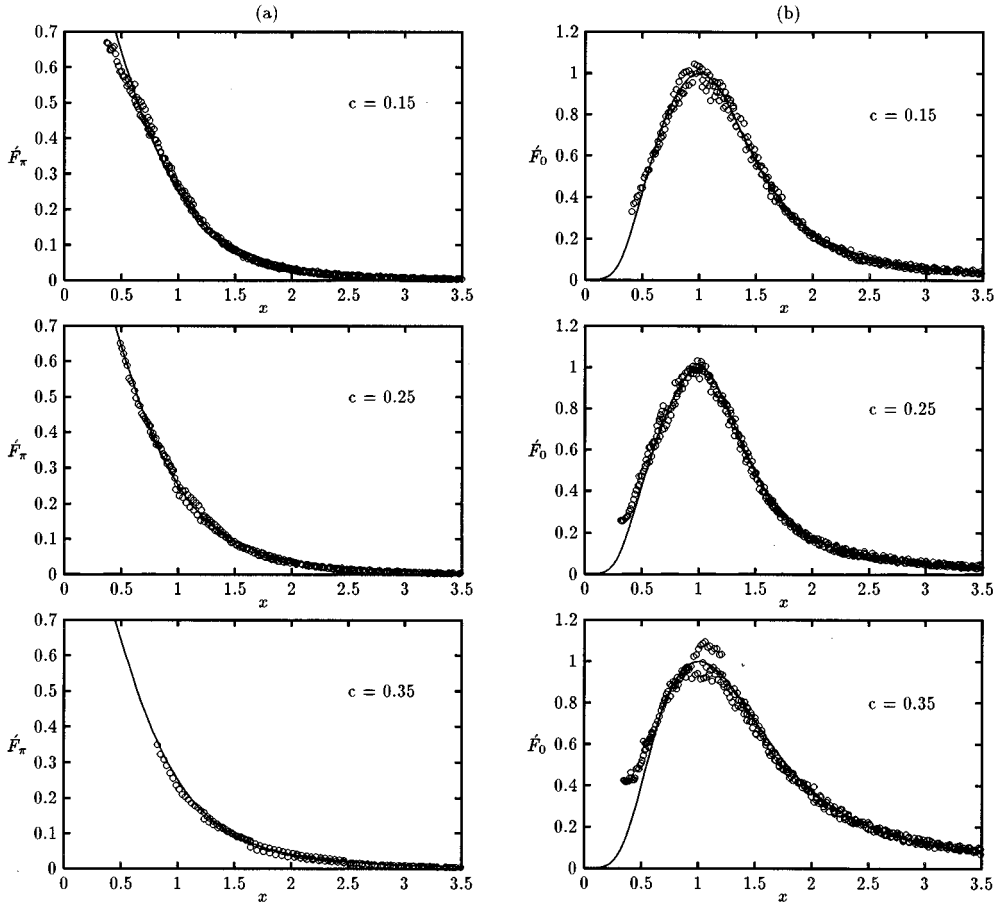

FIG. 6. (a) Scaling of the structure function spherical average for ordering, $F_\pi(k/k_\pi)$ where $k_\pi = a'_\pi(t^{1/3}+b_\pi)$, for $c=0.15$, 0.25, and 0.35. The full line is a fit with Eq. (22). (b) Scaling of the structure function spherical average for decomposition, $F_0(k/k_0)$, where $k_0 = a'_0(t^{1/3}+b_0)$ (at the same three concentrations). The full line is a fit with Eq. (21), with the parameters given in Table II.

have a well defined single maximum by the time $t\sim 10^3$ or 10^4 [see Figs. 4(a) and 4(b)]. Using these functions to compute the moments defined in Eq. (12) we find that the two characteristic dimensions related to ordering and decomposition, $\lambda_\nu(t)$, satisfy[35,9]

$$\lambda_\nu(t) = 2\pi/k_\nu(t) \approx a_\nu(t^{1/3}+b_\nu) \tag{16}$$

for times greater than 10^3. This can be seen in Figs. 5(a) and 5(b), for ordering and decomposition, respectively. The constants a_ν and b_ν are given in Table I. Equation (16) shows that the growth of all characteristic dimensions is consistent with the fimiliar $t^{1/3}$ growth law[8,35] although an unambiguous determination of the growth law exponent would only be possible with much longer runs on a considerably larger lattice.

We now investigate the scaling hypothesis for both functions which requires that $S_\nu(k,t)$ can be written in the form

$$S_\nu(k,t) \approx B_\nu k'_\nu(t)^{-2} F_\nu(k/k'_\nu(t)), \tag{17}$$

where we have used the constancy of the sums in Eqs. (13) and (14); $k'_\nu(t)$ may differ from the previously defined $k_\nu(t)$ by a time-independent (but composition-dependent) factor, i.e.,

$$2\pi/k'_\nu(t) = a'_\nu(t^{1/3}+b_\nu). \tag{18}$$

A standard way to choose the constants a'_0 and B_0 is to require that the scaling function F_0 satisfy the normalization condition

$$\max[F_0(x)] = F_0(1) = 1. \tag{19}$$

This permits comparison of characteristic parameters at different concentrations.

To better locate the maximum of the function $F_0(x)$, we tried various empirical fits starting with a one-parameter fitting expression proposed for decomposition in two dimensions, Eq. (14) in Ref. 9. While this works well for pure segregation and gave a reasonable fit to our data, it appeared to miss the stronger asymmetry, about the maximum, present in our system. This was particularly apparent at $c=0.35$ when the morphology is indeed very different from the pure segregation case. We found by trial and error that the following formula:

$$F_0(x) = \alpha x^4/(\gamma+x^4)[\beta+(x^2-1+\delta)^2]^r, \quad \alpha,\beta,\gamma>0, \tag{20}$$

TABLE II. Parameters a'_ν and B_ν used for the scaling of the structure functions, Eqs. (17) and (18), and parameters β and δ used for the fitting of $F_0(x)$ with Eq. (21), as a function of the concentration of minority atoms, c.

c	a'_π	B_π	a'_0	B_0	β	δ
0.15	0.82	3.1	0.97	0.53	1.47	0.13
0.25	1.01	5.1	0.79	0.75	0.98	0.065
0.35	1.75	6.7	0.65	0.37	3.5	0.55

$r=3/4$, gave a good fit. The form (20) with 3/4 replaced by $(d+1)/4$ is a generalization, satisfying Porod's law $[F_0(x)\sim x^{-(d+1)}$ at $x\to\infty]$,[36] of a heuristic formula suggested in Ref. 10 for 3D alloys (where $d=3$). Definition of the standard form function $F_0(x)$ yields two relations between parameters

$$\alpha=(1+\gamma)(\beta+\delta^2)^r, \quad \gamma=r\delta/(\beta-r\delta+\delta^2) \tag{21}$$

so, two of the four parameters, preferably β and δ, are independent. These were fitted from the data.

For F_π the situation was more difficult, because there was no scaling close to (π,π). The reason for this is that $S(\pi,\pi)$ is related to the (nonconserved) long-range order parameter $[S(\pi,\pi)=N\eta_{\rm lr}^2]$, which depends strongly on how the ordered phase is distributed over the two sublattices. Further away from the (π,π) point, the structure function describes the short-range order, which is not sensitive to the difference between the two sublattices. Because of that, a'_π and B_π were determined by fitting of $F_\pi(x)$ in the region where scaling holds, to the square of the Lorentzian function,

$$F_\pi(x)=1/(1+x^2)^2. \tag{22}$$

As shown in Fig. 6, we observe scaling of both structure functions (for ordering and for decomposition) for times $t\sim10^4$ through $t\sim10^5$. The obtained values for the constants β, δ, a'_ν, and B_ν are given in Table II. We find that a'_π, giving the rate of ordering kinetics, increases while the rate a'_0 of decomposition (coarsening) decreases with the amount of ordered phase at equilibrium. This is presumably due to the very different morphologies at high and low concentrations discussed earlier.

Finally, the dependence of full width at half maximum (FWHM) of the scaling function on the volume fraction of B-rich phase is given in Fig. 7 where it is compared with the $\mathrm{FWHM}_{\rm ferro}$ obtained from simulations on the two-dimensional Ising model with attractive nearest-neighbor interaction between like atoms.[9] The $\mathrm{FWHM}_{\rm ferro}$ is practically temperature independent (for $0.34\leq T/T_c\leq0.8$, T_c being the critical temperature) and symmetric around the volume fraction $f=0.5$. In the present model, however, the scaling function is wider in all cases, indicating a smaller amount of regularity in the positions of the precipitates. Moreover, there is a clear asymmetry between $f\approx0.3$ and $f\approx0.7$, which is not surprising since the morphologies of the two-phase mixtures are also quite different at these compositions (cf. Fig. 2).

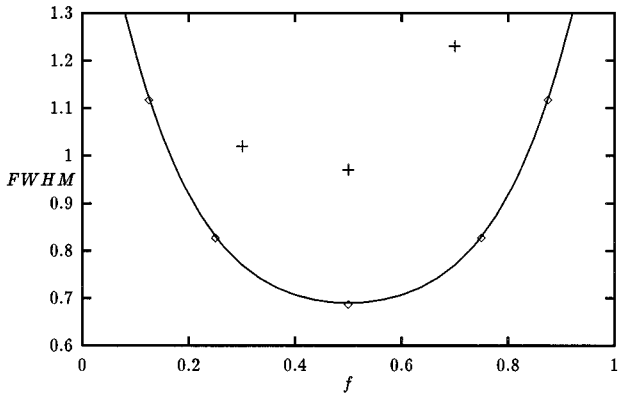

FIG. 7. Full width at half maximum of the scaling function for decomposition normalized according to Eq. (19), as a function of the volume fraction f of the B-rich phase (crosses). Data obtained with a two-dimensional Ising model with attractive nearest-neighbor interaction between like atoms (taken from Ref. 9) are also shown for comparison (diamonds).

V. DISCUSSION

The general picture emerging for the ordering/decomposition process in the present model is that the phase transformation starts with the development of (short-range) order followed by the appearance of well-ordered domains inside a disordered matrix. At this stage, the ordering [as characterized by the short-range order parameter $\eta_{\rm sr}$, Eq. (3)] has reached its maximum value and the further development corresponds to the coarsening of domains by long-range diffusion, much like in a situation where decomposition into two pure (or disordered) phases occurs. The fact that ordering appears prior to decomposition has been observed experimentally[29,30,11–15] and can be explained by the fact that the diffusion of B atoms is required only over short distances for the development of atomic order but needs to cover long distances for the decomposition into phases with different amounts of B atoms.

The coarsening kinetics of the domains, measured by the correlation lengths for decomposition, k_0^{-1}, and for ordering, k_π^{-1}, is consistent with a growth of domain size proportional to $t^{1/3}$, in agreement with experiments on ordered precipitates.[29,38,11–15] This growth law, as well as the observed time scaling of the structure function, are a signature of the coarsening of two-phase structures under the influence of interfacial energy.[9,35,37] The most striking difference between the present case and a conventional coarsening process (with two disordered or pure phases) is the composition dependence of the morphology.

In particular, the lack in symmetry between the cases $c=0.15$ (with volume fraction $f\approx0.3$) and $c=0.35$ (with volume fraction $f\approx0.7$) may be related to the presence of ordered domains of two kinds (on the two sublattices) with some additional positive energy appearing (as pointed out, e.g., in Refs. 29, 30, and 34) on their interface when they are coming in contact due to their growth (antiphase boundary). These antiphase boundaries (APB's) appear to be wetted by the disordered phase which reduces the overall energy of the system. Hence, even though the ordered phase is the majority at $c=0.35$, individual ordered droplets do not join up but

stay separated by narrow channels of disordered phase [see Fig. 2(c)]. The composition-dependent morphology may also be at the origin of the dramatically different behavior of the typical length scales for ordering λ_π and for decomposition λ_0, when the alloy composition is changed.

ACKNOWLEDGMENTS

We thank Sorin Bastea, Claude Laberge, Armen Khachaturyan, and Yunzhi Wang for their help. This work was supported in part by NSF Grant No. NSF-DMR 92-13424, and FWF Grant No. S5601.

[1] J. W. Cahn, Acta Metall. **9**, 795 (1961); **10**, 179 (1962).
[2] A. B. Bortz, M. H. Kalos, J. L. Lebowitz, and M. H. Zendejas, Phys. Rev. B **10**, 535 (1974); J. Marro, A. B. Bortz, M. H. Kalos, and J. L. Lebowitz, *ibid.* **12**, 2000 (1975).
[3] J. D. Gunton, M. San Miguel, and P. S. Sahni, in *Phase Transitions and Critical Phenomena*, edited by C. Domb and J. L. Lebowitz (Academic, New York, 1983), Vol. 8.
[4] K. Binder, in *Materials Science and Technology*, edited by P. Haasen (VCH, Weinheim, 1991), Vol. 5, Chap. 7.
[5] R. Wagner and R. Kampmann, in *Phase Transformations in Materials*, edited by P. Haasen (VCH, Weinheim, 1991), Vol. 5, Chap. 4.
[6] A. G. Khachaturyan, *Theory of Structural Transformations in Solids* (Wiley, New York, 1983).
[7] J. Marro, J. L. Lebowitz, and M. H. Kalos, Phys. Rev. Lett. **43**, 282 (1979); J. L. Lebowitz, J. Marro, and M. H. Kalos, Acta Metall. **30**, 297 (1982); P. Fratzl, J. L. Lebowitz, J. Marro, and M. H. Kalos, *ibid.* **31**, 1849 (1983).
[8] I. M. Lifshitz and V. V. Slyozov, J. Phys. Chem. Solids **19**, 35 (1961); C. Wagner, Z. Elektrochem. **65**, 568 (1961).
[9] P. Fratzl, J. L. Lebowitz, O. Penrose, and J. Amar, Phys. Rev. B **44**, 4794 (1991).
[10] P. Fratzl and J. L. Lebowitz, Acta Metall. **37**, 3245 (1989).
[11] T. Miyazaki, M. Doi, and T. Kozaki, Solid State Phenom. **3**, 158 (1988); T. Miyazaki and M. Doi, Mater. Sci. Eng. A **110**, 175 (1989).
[12] A. Maheshwari and A. J. Ardell, Phys. Rev. Lett. **70**, 2305 (1993).
[13] O. Paris, M. Fährmann, and P. Fratzl, Phys. Rev. Lett. **75**, 3458 (1995).
[14] A. D. Sequeira, H. A. Calderon, G. Kostorz, and J. A. Pedersen, Acta Metall. Mater. **43**, 3427 (1995); **43**, 3441 (1995).
[15] M. Fährmann, P. Fratzl, O. Paris, E. Fährmann, and W. C. Johnson, Acta Metall. Mater. **43**, 1007 (1995).
[16] P. Fratzl, F. Langmayr, G. Vogl, and W. Miekeley, Acta Metall. Mater. **39**, 753 (1991); F. Langmayr, P. Fratzl, G. Vogl, and W. Miekeley, Phys. Rev. B **49**, 11 759 (1994).
[17] J. D. Eshelby, Prog. Solid Mech. **2**, 89 (1961); A. J. Ardell, R. B. Nicholson, and J. D. Eshelby, Acta Metall. **14**, 1295 (1966).
[18] A. Onuki and H. Nishimori, Phys. Rev. B **43**, 13 649 (1991); H. Nishimori and A. Onuki, *ibid.* **42**, 980 (1990).
[19] Y. Wang, L. Q. Chen, and A. G. Khachaturyan, Acta Metall. Mater. **41**, 279 (1993); Y. Wang and A. G. Khachaturyan, *ibid.* **43**, 1837 (1995).
[20] Y. Wang and A. G. Khachaturyan, Scr. Metall. Mater. **31**, 1425 (1994).
[21] W. C. Johnson, Acta Metall. **32**, 465 (1984); T. A. Abinandanan and W. C. Johnson, Acta Metall. Mater. **41**, 17 (1993).
[22] P. W. Voorhees, G. B. McFadden, and W. C. Johnson, Acta Metall. Mater. **40**, 2979 (1992).
[23] K. Kawasaki and Y. Enomoto, Physica A **150**, 463 (1988); Y. Enomoto and K. Kawasaki, Acta Metall. **37**, 1399 (1989).
[24] P. Fratzl and O. Penrose, Acta Metall. Mater. **43**, 2921 (1995).
[25] C. L. Laberge, P. Fratzl, and J. L. Lebowitz, Phys. Rev. Lett. **75**, 4448 (1995).
[26] W. A. Soffa and D. E. Laughlin, Acta Metall. **37**, 3019 (1989).
[27] C. Sagui, A. M. Somoza, and R. C. Desai, Phys. Rev. E **50**, 4865 (1994).
[28] P. S. Sahni, J. D. Gunton, S. L. Katz, and R. H. Timpe, Phys. Rev. B **25**, 389 (1982).
[29] O. Blaschko, R. Glas, and P. Weinzierl, Acta Metall. Mater. **38**, 1053 (1990).
[30] H. Okuda, V. Vezin, K. Osamura, and Y. Amemyia, in *Proceedings of Solid→Solid Phase Transformations*, edited by W. C. Johnson *et al.* (The Minerals, Metals, and Materials Society, Warrendale, PA, 1994), p. 371.
[31] D. P. Landau, J. Appl. Phys. **42**, 1284 (1971).
[32] D. P. Landau, Phys. Rev. Lett. **28**, 449 (1972).
[33] D. de Fontaine, in *Solid State Physics: Advances in Research and Applications*, edited by H. Ehrenreich, F. Seitz, and D. Turnbull (Academic, New York, 1979), Vol. 34, p. 74.
[34] L.-Q. Chen and A. G. Khachaturyan, Acta Metall. Mater. **39**, 2533 (1991).
[35] D. A. Huse, Phys. Rev. B **34**, 7845 (1986).
[36] G. Porod, Kolloid Z. **124**, 83 (1951); **125**, 51 (1952).
[37] N. Akaiwa and P. W. Voorhees, Phys. Rev. E **49**, 3860 (1994).
[38] P. Fratzl and O. Penrose, Acta Mater. **44**, 3227 (1996).